# 4. Modeling of Gravity Attraction

## 4.1. Gravity Anomalies of Bodies with Simple Geometric Shapes

To appreciate the contributions of complex-shaped bodies to gravity anomalies, it is helpful to understand the gravitational effects of bodies with simple geometric shapes. In the following chapter computer programs for the computation of the vertical gravitational effect of simple shaped bodies are presented using the software package MATLAB (Hanselman and Littlefield, 1995).

Throughout the chapter the following notations are used:

- $\Delta g_z$ = vertical gravitational effect of the body
- $\Delta\rho$ = density contrast
- G = gravitational constant.

### 4.1.1. Vertical gravitational attraction of a sphere

The attraction of sphere buried below earth's surface can be viewed in much the same as the attraction of the entire earth from some distance in space; the formula of vertical gravity effect at point P (fig. 4.1a) is (Telford et al., 1981):

$$\Delta g_z = \frac{4\pi G \Delta\rho R^3}{3} \frac{z}{\left(x^2 + z^2\right)^{3/2}} \qquad (4.1)$$

where:

R = radius of sphere (m)

x = horizontal distance from the centre (m)

z = depth of sphere (m)

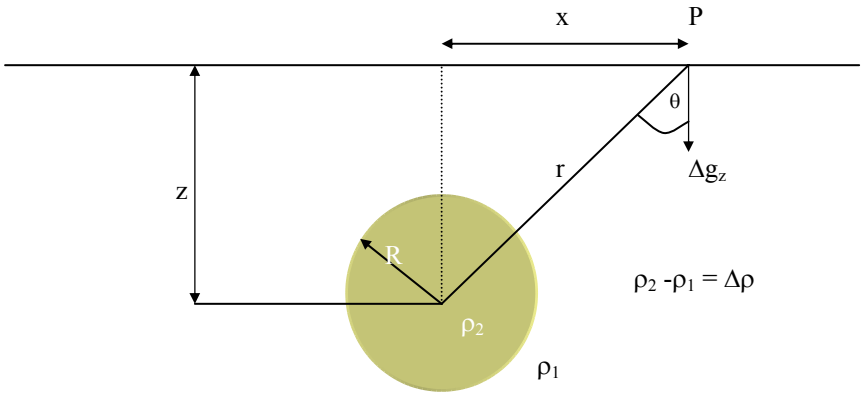


Fig. 4.1a Vertical gravity effect of a sphere at point P.

The change of the vertical gravity effect $\Delta g_z$ with $\Delta\rho$ = 1000 kg/m$^3$, R = 1 m and z = 1 m, 1.1 m and 1.2 m is shown in figure 4.1b; the name of the program is grav_sphere.m (appendix A.1).

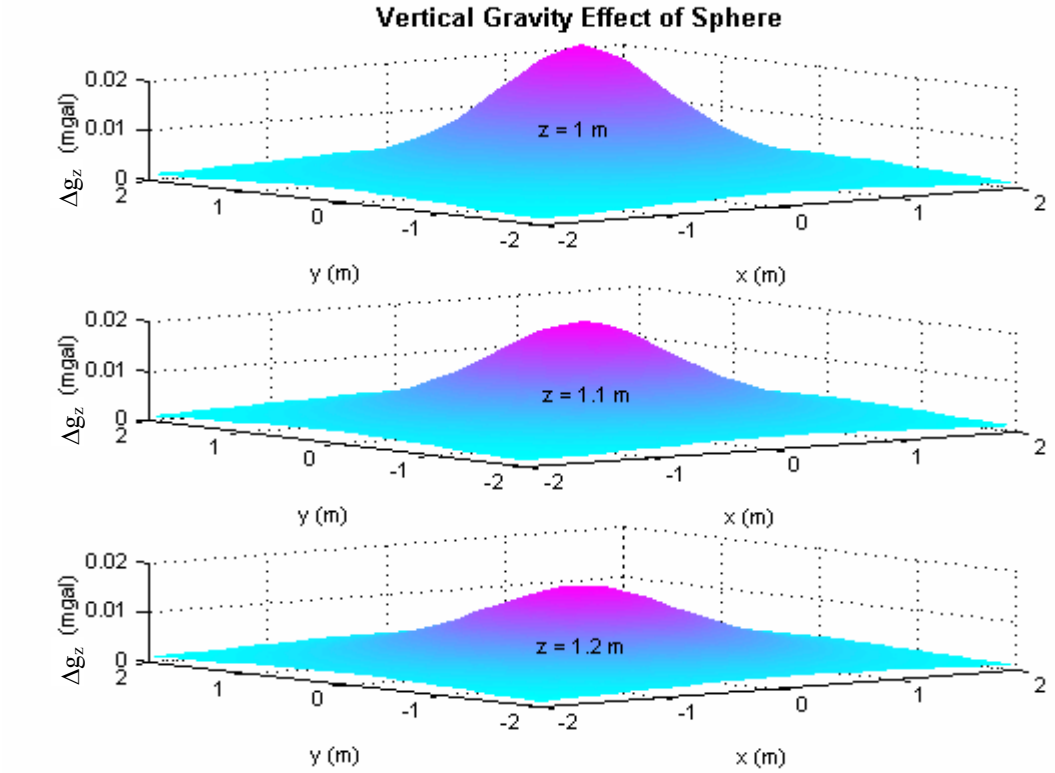


Fig. 4.1b Vertical gravity effect of a sphere with $\Delta\rho$ =1000kg/m$^3$, R=1 m and z = 1, 1.1, 1.2 m.

## 4.1.2. Vertical gravitational attraction of a thin rod

The vertical gravitational attraction $\Delta g_z$ of a thin rod with an inclination $\alpha$ and cross-section $\Delta A$ at point P (fig.4.2a) is (Telford, 1981):

$$\Delta g_z = \frac{G\Delta\rho\Delta A}{x\sin\alpha}\left[\frac{x + z\cot\alpha}{\left(z^2\csc^2\alpha + 2xz\cot\alpha + x^2\right)^{1/2}} - \frac{x + z\cot\alpha + L\cos\alpha}{\left\{\left(L + z\csc\alpha\right)^2 + x^2 + 2x\left(L\cos\alpha + z\cot\alpha\right)\right\}^{1/2}}\right] \quad \text{..... (4.2)}$$

where:

$\Delta A$ = cross-section [m$^2$]

$x$ = horizontal distance from O [m]

$z$ = depth of top thin rod [m]

$\alpha$ = inclination

$L$ = length of thin rod [m]

The change of $\Delta g_z$ for a thin rod with inclination $\alpha$ = 45$^o$, 90$^o$, 135$^o$, $z$ = 1 m, $\Delta\rho$ = 1000 kg/m$^3$, $\Delta A$= 1 m$^2$, L= 100 m is shown in figure 4.2b; the name of the program is grav_thin_rod.m (appendix A.2).

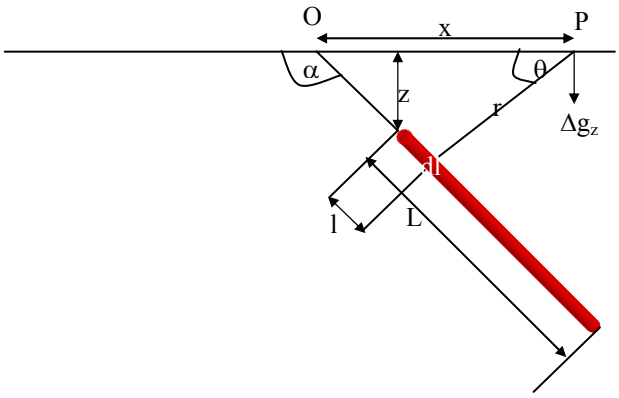


Fig. 4.2a Vertical gravity effect of a thin rod at point P.

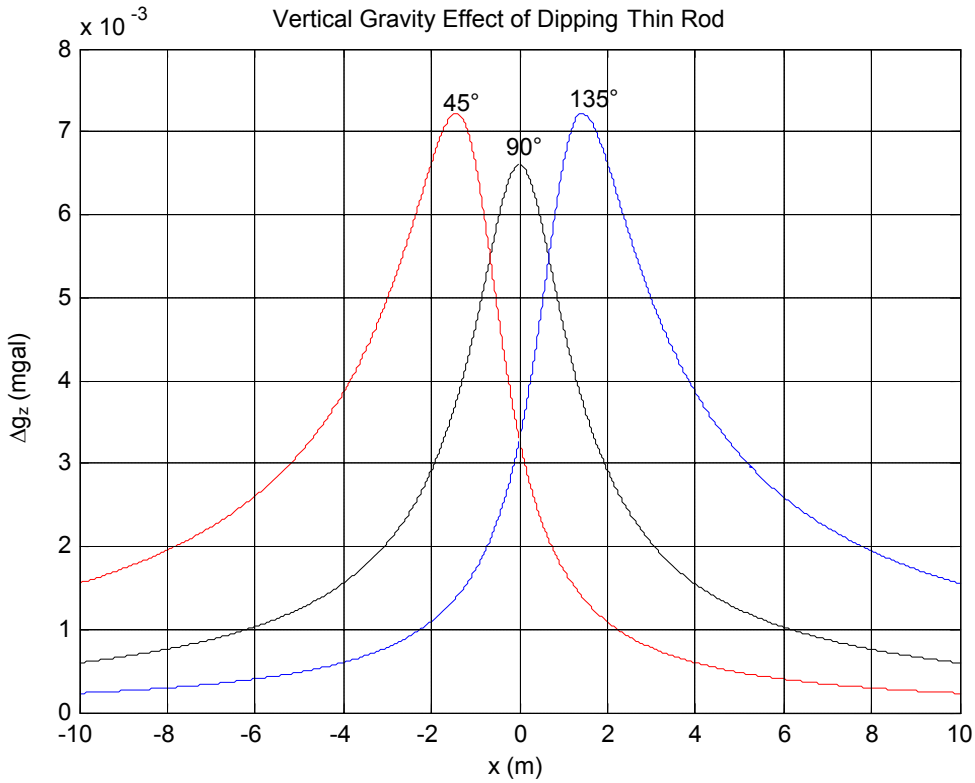


Fig. 4.2b Vertical gravity effect $\Delta g_z$ of a thin rod dipping with inclination $\alpha$ = 45°, 90°, 135°, $z$ = 1 m, $\Delta\rho$ = 1000 kg/m$^3$, $\Delta A$ = 1 m$^2$, L = 100 m.

### 4.1.3. Vertical gravitational attraction of vertical rectangular prism of cross section ΔA

The vertical gravity effect $\Delta g_z$ at point P produced by a prism of cross section ΔA (side small compared to distance to prism axis) (fig. 4.3a) extending from depth $h_1$ to $h_2$ is (Dehlinger, 1978):

$$\Delta g_z = G\frac{\Delta\rho\Delta A}{\left(x^2+y^2\right)^{1/2}}\left(cos\,\alpha_1 - cos\,\alpha_2\right) \qquad (4.3a)$$

or

$$\Delta g_z = G\Delta\rho\Delta A\left(\frac{1}{\left(x^2+y^2+h_1^2\right)^{1/2}} - \frac{1}{\left(x^2+y^2+h_2^2\right)^{1/2}}\right) \qquad (4.3b)$$

where:
ΔA = cross-section [$m^2$]
*x,y* = horizontal distance from P to prism [m]
$h_1$ = depth of prism top [m]
$h_2$ = depth of prism bottom [m]

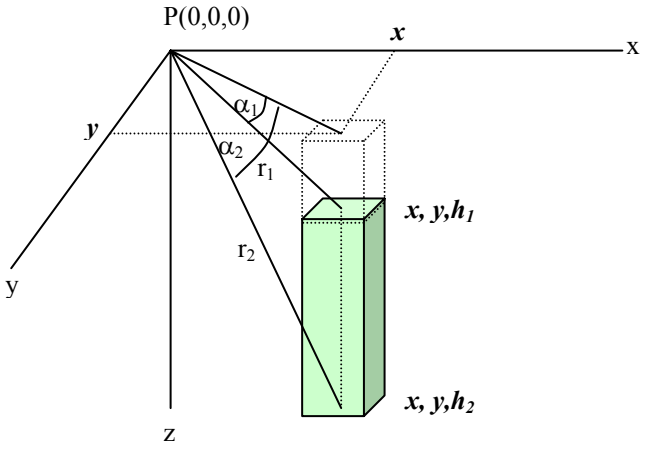


Fig. 4.3a Vertical gravity effect $\Delta g_z$ of a rectangular prism which cross-section ΔA at point P.

The change of the vertical gravity effect $\Delta g_z$ of a vertical rectangular prism with depth $h_1$ = 1 m and $h_2$ = 100 m, $\Delta\rho$ = 1 g/$cm^3$, ΔA= 1 $m^2$ (V = 99 $m^3$) dependent on x and y is shown in fig. 4.3b; the name of the program is grav_prism.m (appendix A.3).

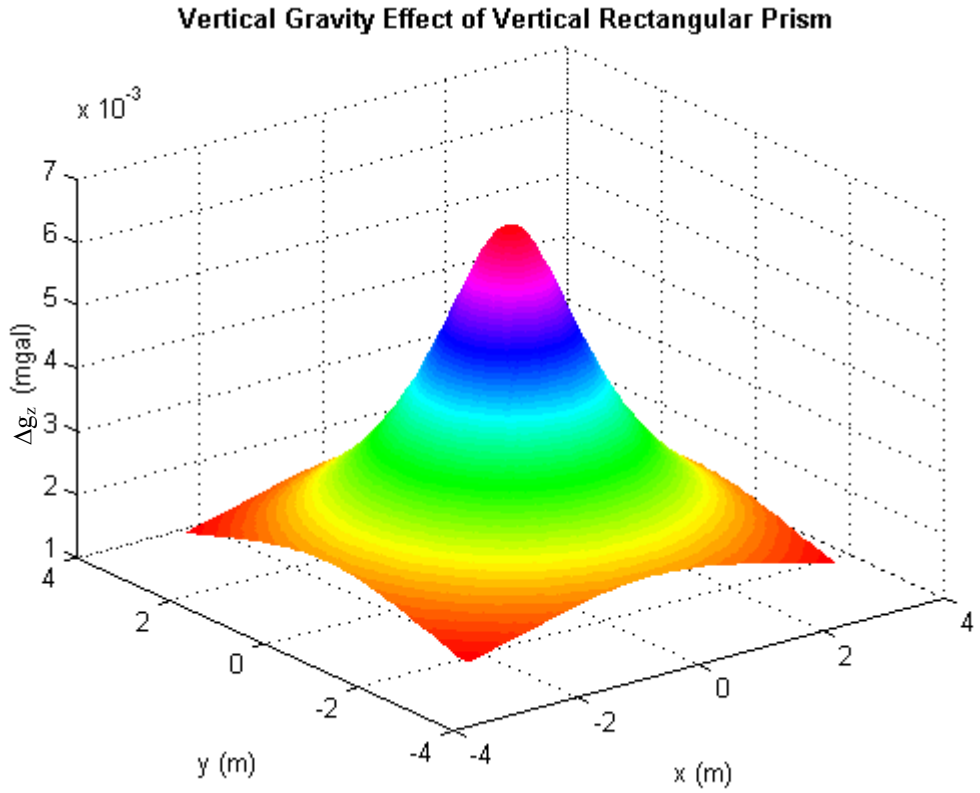


Fig. 4.3b Vertical gravity effect $\Delta g_z$ of a prism with depth $h_1$ = 1 m and $h_2$ = 100 m, $\Delta\rho$ = 1000 kg /m$^3$, $\Delta A$= 1 m$^2$.

### 4.1.4. Vertical gravitational attraction of vertical rectangular parallelepiped

The shape of an irregular three-dimensional body can be approximated by rectangular parallelepipeds, especially cubes. The vertical gravity effect $\Delta g_z$ of a parallelepiped produced at a corner P of the body with sides x, y and z (fig. 4.4a) is (Talwani, 1973):

$$\Delta g_z = G\Delta\rho\left\{z_1\left[\frac{\pi}{2} - \sin^{-1}(\cos\beta\cos\lambda) - \sin^{-1}(\cos\beta\sin\lambda)\right] + \frac{x_1}{2}\ln\left[\frac{(r_1 - y_1)(r_z + y_1)}{(r_1 + y_1)(r_z - y_1)}\right] + \frac{y_1}{2}\ln\left[\frac{(r_1 - x_1)(r_z + x_1)}{(r_1 + x_1)(r_z - x_1)}\right]\right\} \quad (4.4)$$

where:

$r_1 = (x_1^2 + y_1^2 + z_1^2)^{1/2}$

$r_x = (y_1^2 + z_1^2)^{1/2}$ $\quad r_y = (x_1^2 + z_1^2)^{1/2}$ $\quad r_z = (x_1^2 + y_1^2)^{1/2}$

$\cos l = x_1/r_1$ $\quad \cos m = y_1/r_1$ $\quad \cos n = z_1/r_1$

$\cos\alpha = z_1/r_x$ $\quad \cos\beta = z_1/r_y$ $\quad \cos\lambda = y_1/r_z$ $\quad \sin\lambda = x_1/r_z$

This equation can be applied successively to compute the vertical gravity effect of a parallelepiped where P is not at a corner (fig. 4.4b).

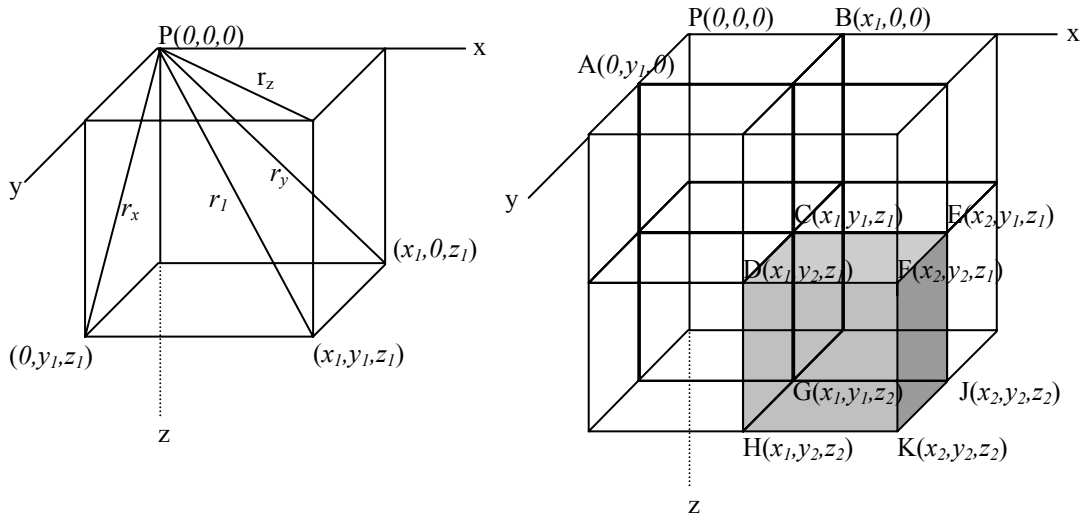


(a) (b)

Fig. 4.4 Bodies for computing vertical gravity effect at P: (a). rectangular parallelepiped with one corner at origin of coordinates, (b). rectangular parallelepipeds; the shaded parallelepiped does not have corner at the origin.

The vertical gravity effect of the rectangular parallelepiped CK is the sum and difference of eight rectangular parallelepipeds, whereby seven have a corner at P (Talwani, 1973). Thus:

$$(\Delta g)_{CK} = (\Delta g)_{PK} - (\Delta g)_{PJ} + (\Delta g)_{PG} - (\Delta g)_{PH} - (\Delta g)_{PF} + (\Delta g)_{PE} - (\Delta g)_{PC} + (\Delta g)_{PD} \qquad (4.5)$$

Fig. 4.4c shows the change of vertical gravity effect $\Delta g_z$ of such a general rectangular parallelepiped. The parameters are $z_1 = 1$ m, $z_2 = 2$ m, $x_2 - x_1 = 1$ m, $y_2 - y_1 = 1$ m ($V = 1$ m$^3$); the horizontal distances of $x_1$, $x_2$, $y_1$, $y_2$ are varying toward the origin, $\Delta\rho = 1000$ kg/m$^3$. The name of the program is grav_rectangular.m (appendix A.4).

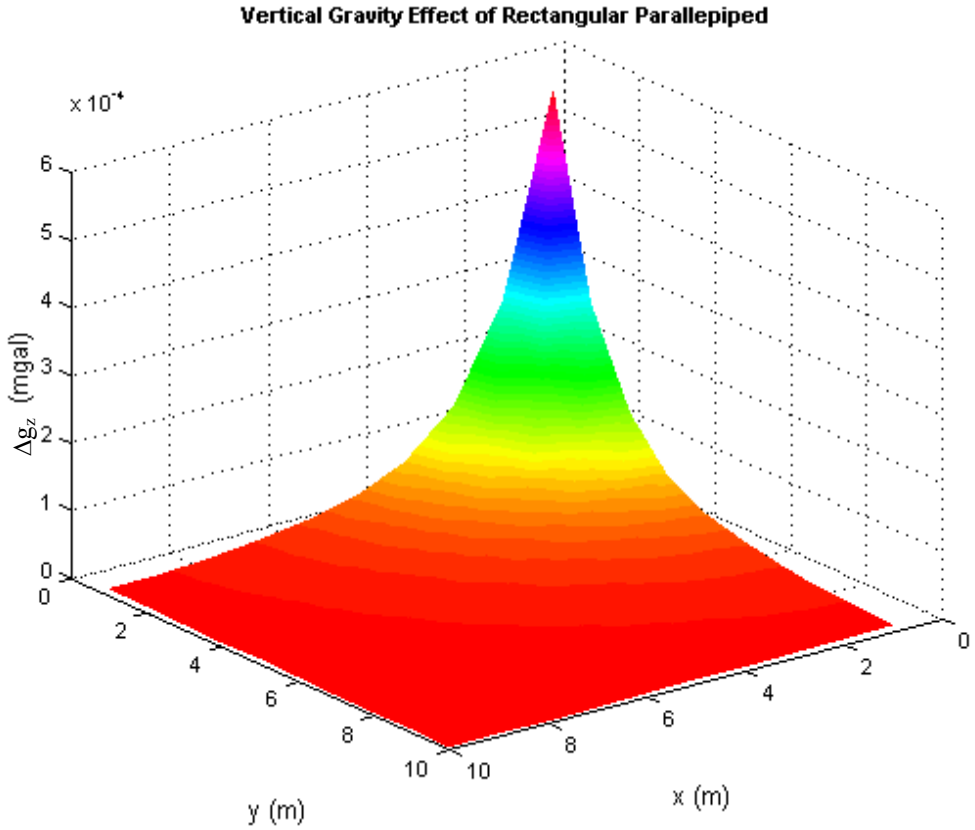


Fig. 4.4c Vertical gravity effect of rectangular parallelepiped with none corner at the origin; $z_1$ = 1 m, $z_2$ = 2 m, $x_2 - x_1$ = 1 m, $y_2 - y_1$ = 1 m; the horizontal distances of $x_1$, $x_2$, $y_1$, $y_2$ are varying toward origin, $\Delta\rho$ = 1000 kg/m$^3$.

## 4.1.5. Vertical gravitational attraction of thick vertical cylinder

The vertical gravity effect $\Delta g_z$ at a point P on the axis of a vertical cylinder (fig. 4.5a) is (Telford et al., 1981):

$$\Delta g_z = 2\pi G\Delta\rho\left(L + \sqrt{z^2 + R^2} - \sqrt{(z+L)^2 + R^2}\right) \qquad (4.6a)$$

where:
$R$ = radius of cylinder (m); $z$ = depth of cylinder (m); $L$= length of cylinder (m).

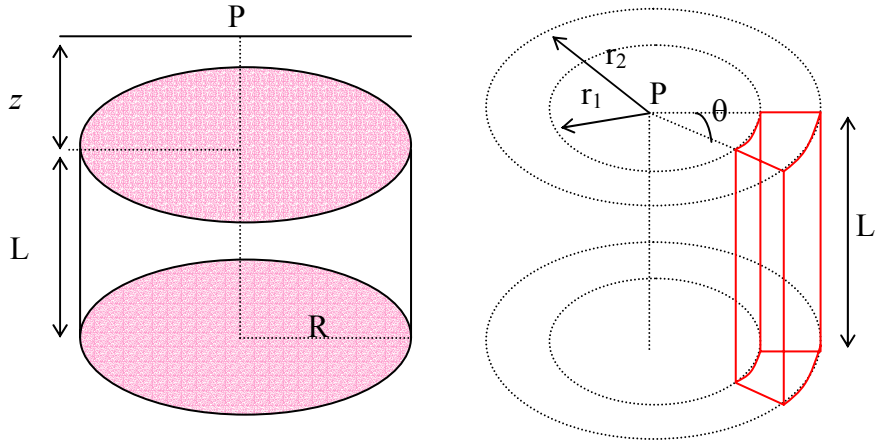


(a) (b)

Fig. 4.5 (a) Vertical gravity effect $\Delta g_z$ of a vertical cylinder on the axis; (b) of cylindrical slice.

There are several significant limiting cases of this formula.
1. If $R \to \infty$, we obtain the infinite horizontal slab (Bouguer plate of thickness L):

$$\Delta g_z = 2\pi G \Delta \rho L \tag{4.6b}$$

2. The vertical gravitational effect $\Delta g_z$ of a sector of the cylinder (fig. 4.4b) is:

$$\Delta g_z = G\Delta\rho\theta\left(\sqrt{r_1^2 + L^2} - \sqrt{r_2^2 + L^2} + (r_2 - r_1)\right) \tag{4.6c}$$

where:
$r_1$ = inner radius (m)
$r_2$ = outer radius (m)
$\theta$ = sector angle (radian)
This is the formula of the terrain correction (see 3.2.4), where L - the depth of the sector - corresponds to the difference between the height of the station and the average elevation in the sector.
3. If z = 0, the cylinder outcrops:

$$\Delta g_z = 2\pi G \Delta \rho \left(L + R - \sqrt{L^2 + R^2}\right) \tag{4.6d}$$

4. If $L \to \infty$, equation 4.6a becomes:

$$\Delta g_z = 2\pi G \Delta \rho \left(\sqrt{z^2 + R^2} - z\right) \tag{4.6e}$$

When $L >> z$, (that means the cylinder length is considerably larger than the depth z of the top of the cylinder), equation 4.6e can be used to compute the gravity effect for a station P off-axis using the well-known methods of solving Laplace's equation. Since $\Delta g_z$ satisfies Laplace's equation, $\Delta g_z$ can be expressed for $r > z > R$ in a series of Legendre polynomials of the form (fig. 4.6a):

$$\Delta g_z(r,\theta) = k\sum_{n=0}^{\infty} b_n r^{-(n+1)} P_n(\cos\theta) \tag{4.7}$$

where:
$k = 2\pi G\Delta\rho$
$b_n$ = coefficients
$P_n(\cos\theta)$ = Legendre polynomials
$r^2 = x^2 + z^2$
$\tan\theta = x/z$

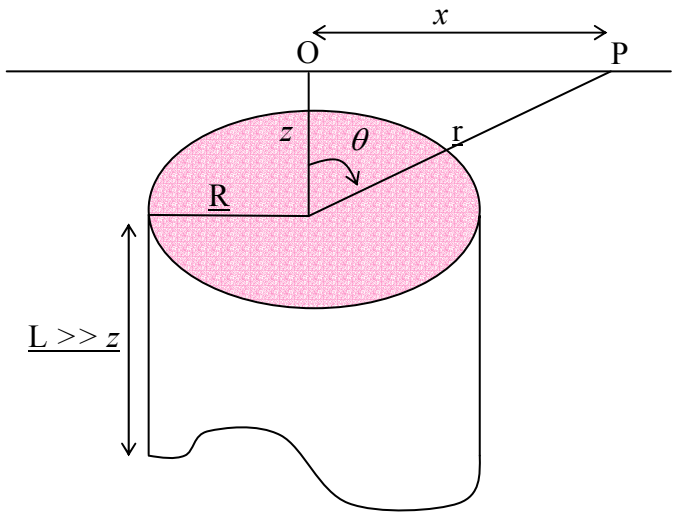


Fig. 4.6a Vertical gravity effect of the thick vertical cylinder at an arbitrary point P.

On the axis $\theta = 0$, $r = z$, the series reduces to

$$\begin{aligned}\Delta g_z &= 2\pi G\Delta\rho\left(\frac{b_0P_0}{z}+\frac{b_1P_1}{z^2}+\frac{b_2P_2}{z^3}+\frac{b_3P_3}{z^4}+\ldots\right)\\ &= 2\pi G\Delta\rho\left(\frac{b_0}{z}+\frac{b_1}{z^2}+\frac{b_2}{z^3}+\frac{b_3}{z^4}+\ldots\right)\end{aligned} \tag{4.8}$$

where:

$P_0, P_1, P_2, \ldots = 1$ (Legendre polynomials for $\theta = 0$).

This result must be the same as that given by equation 4.6e; expanding this equation in terms of R/Z with binomial series equation (4.8) becomes

$$\begin{aligned}\Delta g_z &= 2\pi G\Delta\rho\left(z\sqrt{1+\frac{R^2}{z^2}}-z\right)\\ &= 2\pi G\Delta\rho\left(\frac{R^2}{2z}-\frac{R^4}{8z^3}+\frac{R^6}{16z^5}-\frac{5R^8}{128z^7}+\frac{7R^{10}}{256z^9}+\ldots\right)\end{aligned} \tag{4.9}$$

Equating the coefficients of the two series (equations 4.8 and 4.9) delivers

$b_n = 0$, *if* n is odd, and

$$b_0 = \frac{R^2}{2},\ b_2 = -\frac{R^4}{8},\ b_4 = \frac{R^6}{16},\ b_6 = -\frac{5R^8}{128},\ b_8 = \frac{7R^{10}}{256}\ \ldots$$

The expression $\Delta g_z(r,\theta)$ for an off-axis point P is then

$$\Delta g_z(r,\theta) = 2\pi G\Delta\rho R\left(\frac{1}{2}\left(\frac{R}{r}\right) - \frac{1}{8}\left(\frac{R}{r}\right)^3 P_2(\cos\theta) + \frac{1}{16}\left(\frac{R}{r}\right)^5 P_4(\cos\theta) - \right.$$
$$\left. - \frac{5}{128}\left(\frac{R}{r}\right)^7 P_6(\cos\theta) + \frac{7}{256}\left(\frac{R}{r}\right)^9 P_8(\cos\theta) - \cdots\right) \tag{4.10}$$

Equation 4.10 can be rewritten to resemble equation 4.2 for the long thin rod. By inserting $r = \sqrt{x^2 + y^2}$ , $\Delta g_z(r,\theta)$ can be expressed as

$$\Delta g_z(r,\theta) = \pi G\Delta\rho R^2\left(\frac{1}{\left(x^2+z^2\right)^{\frac{1}{2}}} - \frac{R^2 P_2(\cos\theta)}{4\left(x^2+z^2\right)^{\frac{3}{2}}} + \frac{R^4 P_4(\cos\theta)}{8\left(x^2+z^2\right)^{\frac{5}{2}}} - \right.$$
$$\left. - \frac{5R^6 P_6(\cos\theta)}{64\left(x^2+z^2\right)^{\frac{7}{2}}} + \frac{7R^8 P_6(\cos\theta)}{128\left(x^2+z^2\right)^{\frac{9}{2}}} - \cdots\right) \tag{4.11}$$

This equation gives more precise results then equation 4.2, when the rod is vertical, although the difference between the two solutions is negligible, if $z >> 2R$.
A more useful result for the same thick cylinder can be developed when z < R: expanding equation 4.6e in terms of $z/R$ rather than $R/z$:

$$\Delta g_z = 2\pi G\Delta\rho\left(R\sqrt{1+\frac{z^2}{R^2}} - z\right)$$
$$= 2\pi G\Delta\rho R\left(1 - \frac{z}{R} + \frac{z^2}{2R^2} - \frac{z^4}{8R^4} + \frac{z^6}{16R^6} - \frac{5z^8}{128R^8} + \frac{7z^{10}}{256R^{10}} + \cdots\right) \tag{4.12}$$

Within the interval $z << r << R$ the series is developed to an off-axis series:

$$\Delta g_z(r,\theta) = k\sum_{m=0}^{\infty} a_m r^m P_m(\cos\theta)$$
$$= k\left(a_0 + a_1 r P_1(\cos\theta) + a_2 r^2 P_2(\cos\theta) + a_3 r^3 P_3(\cos\theta) + \cdots\right) \tag{4.13}$$

Equating coefficients on the axis ($\theta = 0$, $r = z$) give:

$$a_0 = R,\ a_1 = -1,\ a_2 = \frac{1}{2R},\ a_3 = a_5 = a_7 = \cdots = a_{2n+1} = 0,\ a_4 = -\frac{1}{8R^3},\ a_6 = \frac{1}{16R^5},$$
$$a_8 = -\frac{5}{128R^7},\ a_{10} = \frac{7}{256R^9} \ldots$$

Thus, for points off the cylinder axis the expression becomes for $z \le r \le R$:

$$\Delta g_z(r,\theta) = 2\pi G\Delta\rho R\left(1-\left(\frac{r}{R}\right)P_1(\cos\theta)+\frac{1}{2}\left(\frac{r}{R}\right)^2 P_2(\cos\theta)-\frac{1}{8}\left(\frac{r}{R}\right)^4 P_4(\cos\theta)+\right.$$
$$\left.+\frac{1}{16}\left(\frac{r}{R}\right)^6 P_6(\cos\theta)-\frac{5}{128}\left(\frac{r}{R}\right)^8 P_8(\cos\theta)+\frac{7}{256}\left(\frac{r}{R}\right)^{10} P_{10}(\cos\theta)-\cdots\right) \quad (4.14)$$

If $R$ is between $r$ and $z$, that is $r > R > z$, different series have to be used, which turns out to be identical in form with equation 4.10; writing $\Delta g_z'(r,\theta)$ to avoid confusion with $\Delta g_z(r,\theta)$ of equation 4.14, we get:

$$\Delta g_z'(r,\theta) = 2\pi G\Delta\rho R\left(\frac{1}{2}\left(\frac{R}{r}\right)-\frac{1}{8}\left(\frac{R}{r}\right)^3 P_2(\cos\theta)+\frac{1}{16}\left(\frac{R}{r}\right)^5 P_4(\cos\theta)-\right.$$
$$\left.-\frac{5}{128}\left(\frac{R}{r}\right)^7 P_6(\cos\theta)+\frac{7}{256}\left(\frac{R}{r}\right)^9 P_8(\cos\theta)-\cdots\right) \quad (4.15)$$

Fig. 4.6b shows $\Delta g_z$ of the thick vertical cylinder dependent on the position of point P. The parameters are $R$ = 5 m, $z$ = 1 m, $\Delta\rho$ = 1000 kg/m$^3$. The name of the program is grav_cylinder_1.m (appendix A.5).

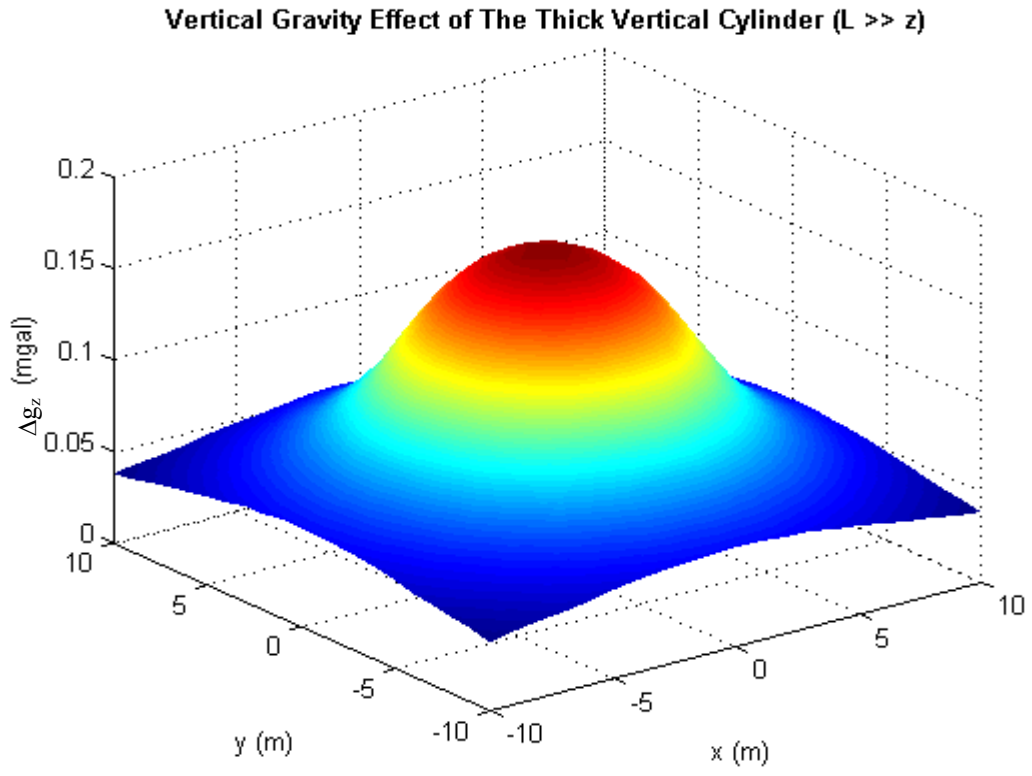


Fig. 4.6b Vertical gravity effect of the thick vertical cylinder for L >> z.

Another way to calculate the gravitational attraction of rotational bodies on a point that lies away from the axis of symmetry is to use series in term of spherical functions (Lewi, 1997). The vertical gravity effect of a vertical cylinder at an arbitrary point (fig. 4.7) using solid spherical functions (Belikov, 1987) is:

$$\Delta g_{z,cyl} = \frac{\partial \upsilon_{cyl}}{\partial z} = \pi R^2 G \Delta\rho \sum_{n=0}^{\infty} \frac{\left(\frac{1}{4}\right)_n \left(\frac{3}{4}\right)_n}{(1)_n (2)_n} \left[\varphi_n(z-l) - \varphi_n(z+l)\right] \tag{4.16}$$

where

$$\varphi_n(z) = \frac{1}{\sqrt{z^2 + X^2 + R^2}} \left[\frac{4R^2X^2}{\left(z^2 + X^2 + R^2\right)}\right]^n \sum_{k=0}^{\infty} \frac{\left(2n + \frac{1}{2}\right)_k}{(n+2)_k} \left(\frac{R^2}{z^2 + X^2 + R^2}\right)^k$$

$\upsilon_{cyl}$ = gravitational potential of the cylinder
$\Delta g_{z,cyl}$ = the vertical component of the gravitational attraction of the vertical cylinder at an arbitrary point
$(x)_n$ = $x(x+1)(x+2)(x+3) \ldots (x+n-1)$
$R$ = radius of the cylinder
$X$ = horizontal distance between the centre of the cylinder and point P
$z$ = vertical distance between the centre of the cylinder and point P
$2l$ = height of the cylinder

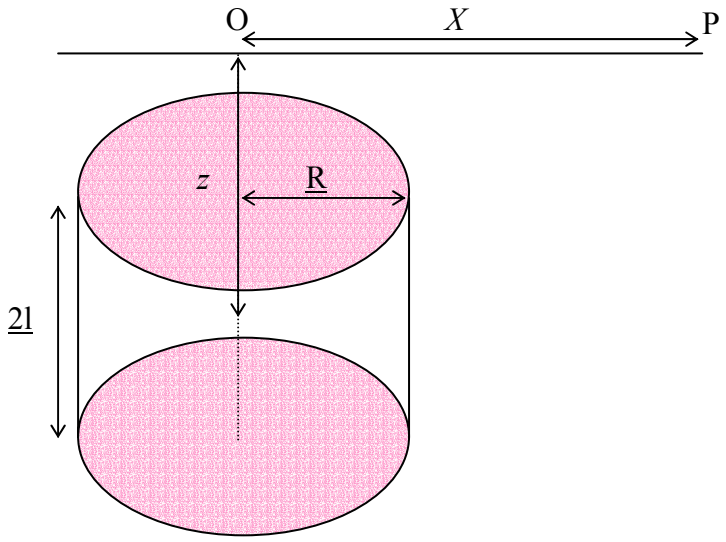


Fig. 4.7 Vertical gravity effect of a vertical cylinder at any arbitrary point P.

The name of the program to calculate equation 4.16 is grav_cylinder_2.m (appendix A.6).
To test grav_cylinder_1.m and grav_cylinder_2.m, we compare them with the vertical gravity effect of a point at the axis (equation 4.6.a). Figure 4.8a shows the vertical gravity effect of the thick vertical cylinder calculated by program grav_cylinder_1.m and grav_cylinder_2.m. The parameters of the cylinder are R = 5 m, z = 1 m, $\Delta\rho$ = 1 g/cm$^3$, l = 5000m. Maximum order of Legendre polynomials used in grav_cylinder_1.m is $P_{2001}(cos\theta)$ and maximum degree of binomials is $b_{1000}$. Summation in grav_cylinder_2.m runs up to 100. Differences of the results grav_cylinder_1.m -grav_cylinder_2.m and the result on the axis (equation 4.6a) are shown in fig. 4.8b.

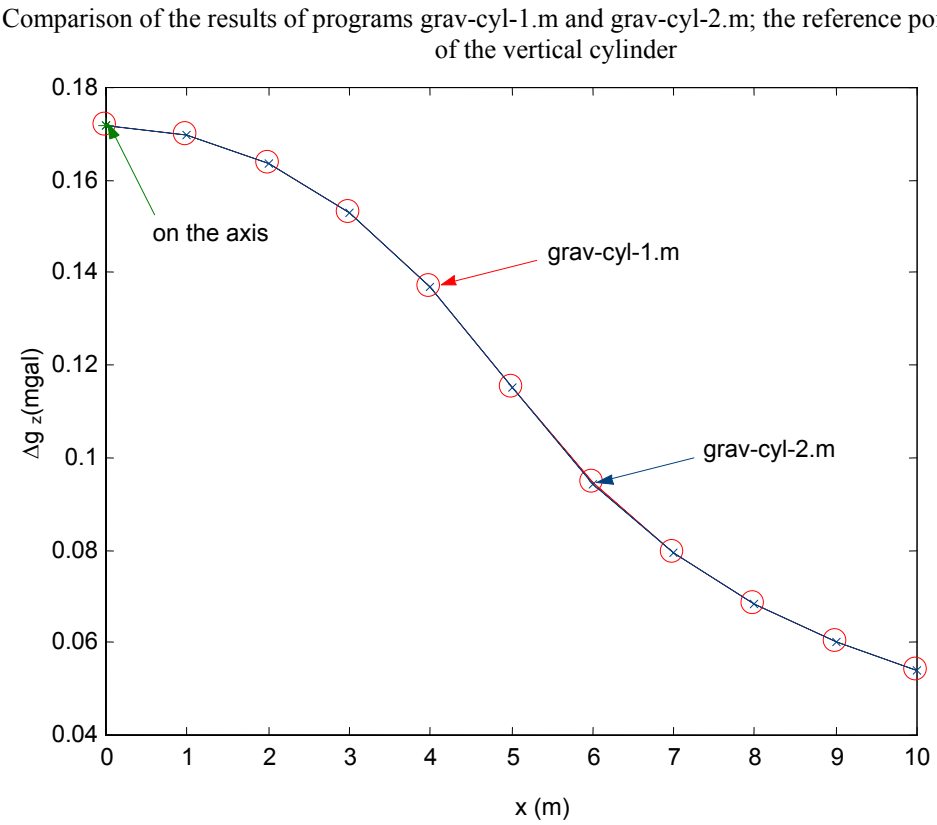


Fig. 4.8a. The vertical gravity effects of the thick vertical cylinder calculated by the programs grav_cylinder_1.m and grav_cylinder_2.m.

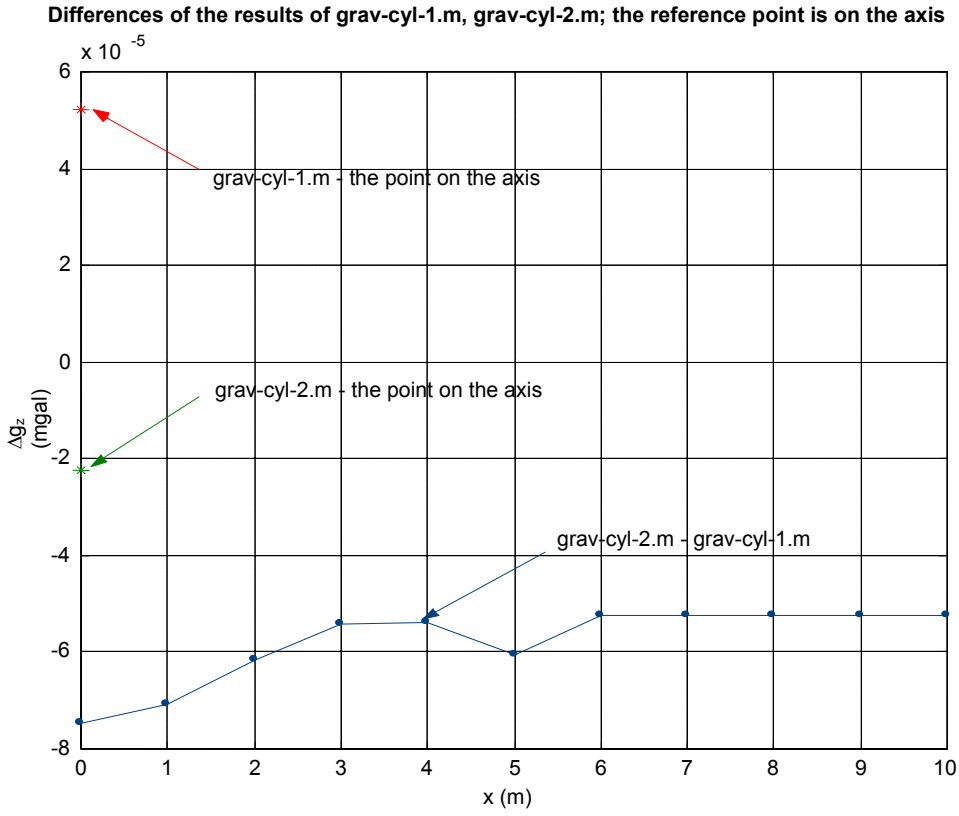


Fig. 4.8b Differences of the results of grav_cylinder_1.m and grav_cylinder_2.m; the reference point is on the axis.

## 4.2. Alternative Model of Merapi Volcano

The schematic surface forms and subsurface structures of various volcanic features are shown in figure 4.9 (Decker and Decker, 1989). Post-mortems of these rocks show that the dikes and pipes of chilled magma often connect surface vents to larger storage chambers of molten rock. The depth of magma chambers is between 2 to 10 kilometres beneath the surface.

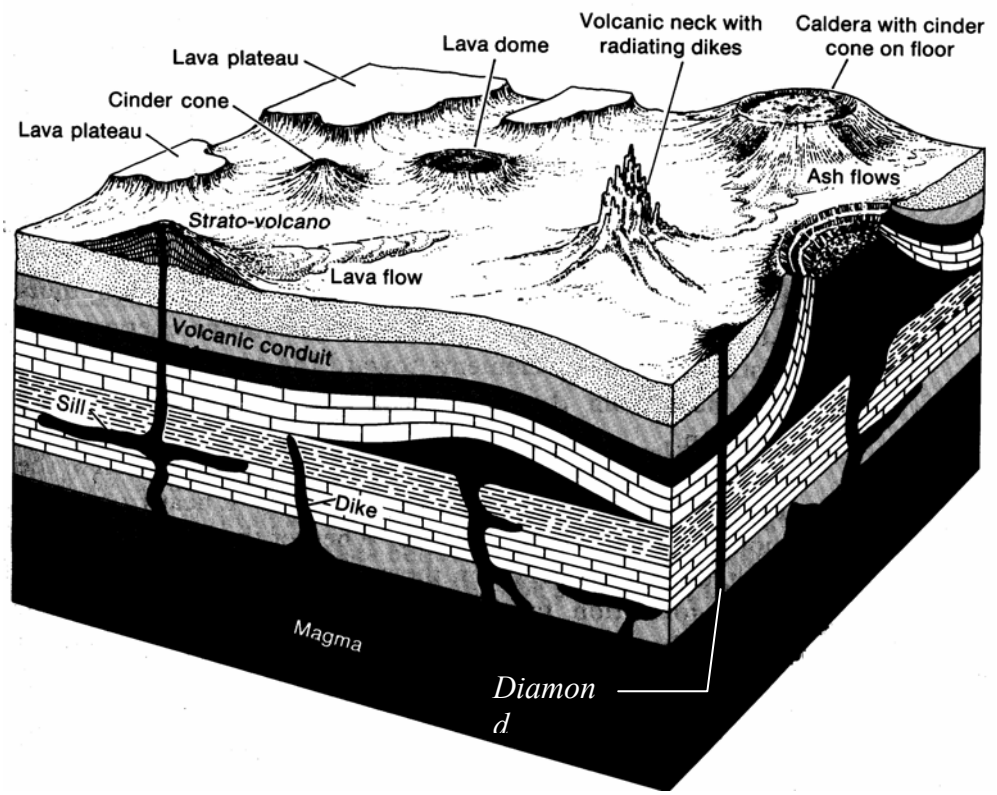


Fig. 4.9 Schematic diagram of the surface forms and subsurface structure of various volcanic features (R.G. Schmidt and H. R. Shaw, 1972).

Merapi itself is a stratovolcano with a summit lava dome. For Merapi the following models are assumed.

### 4.2.1. Combination-model: sphere and dipping thin rod

A possible model of Merapi volcano is a so called combination-model of sphere and dipping thin rod representing the magma chamber and the conduit (fig. 4.10). The gravitational attraction of three bodies has to be calculated:

- sphere filled with magma
- dipping thin rod filled with magma
- dipping thin rod filled with air

We have to notice the altitude z of observation position, whether it is higher or less than the horizon $z_b$ of magma filled in the thin rod.

The vertical gravity effect of a sphere filled with magma is according (4.1)

$$\Delta g_{z\_s} = \frac{4\pi G \Delta\rho R^3}{3} \frac{z_s}{\left(x_s^{\,2} + z_s^{\,2}\right)^{3/2}}$$

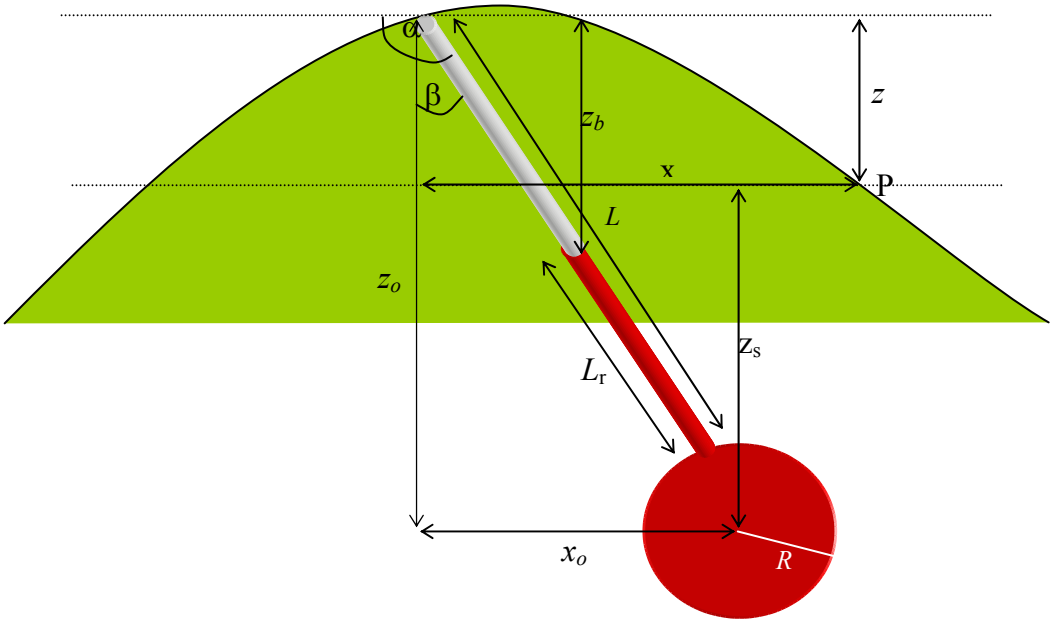


Fig.4.10. Combination model of sphere and dipping thin rod.

To calculate gravity effect of thin rod dipping, we get for the boundary conditions:

**If $z_b > z$**

- Vertical gravity effect of dipping thin rod filled with magma

$$\Delta g_{z\_rm} = \frac{G\Delta\rho\Delta A}{x_{rm}\sin\alpha}\left[\frac{x_{rm} + z_{rm}\cot\alpha}{\left(z_{rm}^{\,2}\csc^2\alpha + 2x_{rm}z_{rm}\cot\alpha + x^2\right)^{1/2}} - \frac{x_{rm} + z_{rm}\cot\alpha + L_{rm}\cos\alpha}{\left\{\left(L_{rm} + z_{rm}\csc\alpha\right)^2 + x_{rm}^{\,2} + 2x_{rm}\left(L_{rm}\cos\alpha + z_{rm}\cot\alpha\right)\right\}^{1/2}}\right] \quad \text{..... (4.17a)}$$

where:

$\Delta g_{z\_rm}$ = vertical gravity effect of a thin rod dipping with inclination α (mgal)
$\Delta A$ = cross-section ($m^2$)
$\alpha = \beta + \pi/2$, inclination ($^o$)
$L$ = length of thin rod (m)
$L_{rm}$ = length of thin rod filled with magma (m)
$z_{rm} = (L - L_{rm})\ cos\ \beta - z$
$x_{rm} = x - (z\ tan\ \beta)$

- Vertical gravity effect of thin dipping rod filled with air

$$\Delta g_{z\_ra} = \frac{G\Delta\rho\Delta A}{x_{ra}\sin\alpha}\left[\frac{x_{ra} + z_{ra}\cot\alpha}{\left(z_{ra}^{\,2}\csc^2\alpha + 2x_{ra}z_{ra}\cot\alpha + x^2\right)^{1/2}} - \frac{x_{ra} + z_{ra}\cot\alpha + L_{ra}\cos\alpha}{\left\{\left(L_{ra} + z_{ra}\csc\alpha\right)^2 + x_{ra}^{\,2} + 2x_{ra}\left(L_{ra}\cos\alpha + z_{ra}\cot\alpha\right)\right\}^{1/2}}\right]$$

..... (4.17b)

In this case, we split the integration boundaries:
The parameters of a thin rod dipping below z are:

$z_{ra} = 0$
$x_{ra} = x - (z \tan \beta)$
$L_{ra} = L - L_{rm} - ((z \tan \beta)^2 + z^2)^{1/2}$

The parameters of a thin rod dipping above z are:

$z_{ra} = 0$
$x_{ra} = -(x - (z \tan \beta))$
$L_{ra} = ((z \tan \beta)^2 + z^2)^{1/2}$

The sign of vertical gravity effect of thin rod dipping above z is negative.

**If $z_b \leq z$**

- Vertical gravity effect of a dipping thin rod filled with magma is calculated according equation 4.17a.
  In this case, we split again the integration boundaries:
  The parameters of a thin rod dipping below z are:
  $z_{rm} = 0$
  $x_{rm} = x - (z \tan\beta)$
  $L_{rm} = L - ((z \tan \beta)^2 + z^2)^{1/2}$

  The parameters of a thin rod dipping above z are:
  $z_{rm} = 0$
  $x_{rm} = -(x - (z \tan\beta))$
  $L_{rm} = ((z \tan \beta)^2 + z^2)^{1/2} - (L - L_{rm})$
  The sign of vertical gravity effect of the thin rod dipping above z is negative.

- Vertical gravity effect of dipping thin rod filled with air using equation 4.17b where:
  $z_{ra} = \{((z \tan \beta)^2 + z^2)^{1/2} - (L - L_{rm})\} \cos \beta$
  $x_{ra} = -(x - (z \tan \beta))$
  $L_{ra} = L - L_{rm}$
  The sign of gravity effect of a thin rod dipping above z is negative.

The name of the program for this model is grav_sphere_rod.m (appendix A.7).
As examples in Fig. 4.11 the changes of vertical gravity attraction of a pipe filled with magma at different locations are shown. The locations are identical to the stations JRA15, JRA100, IPU0 and JRA13 of the gravity repetition network at Merapi, which is described in more detail in chapter 5.
This model assumed that

- $x_o = 2000$ m
- $z_0 = 8600$ m
- $R_{sphere} = 137$ m (Beauducel and Cornet, 1999);
- $\rho_{magma} = 2400$ kg/m$^3$
- $\rho_{\text{marine sediment}} = 2100$ kg/m$^3$ (Ritter, A., 1999)

- $\rho_{air} = 0.001293$ g/cm$^3$;
- $r_{rod} = 20$ m.

The centre of the top rod is approximately at the summit of Merapi (20 m toward the south of the station JRA13).

The vertical gravity changes are plotted in fig. 4.11 dependent on the length of the magma pipe for the different summit stations. Fig. 4.12 shows the contour map of vertical gravity changes at station JRA15 dependent on the length of magma in the pipe. The green contour line represents the gravity changes between campaign Aug. 1999 – Aug. 1997 (55.6 μgal); this contour line allows analyzing the movement of magma in the pipe. The name of contour map program is isomap1.m (appendix A.8). These computation and contour map are developed to determine the height of magma in the rod or cylinder, which are representing the volcano's voids; we can look further in the chapter 7.

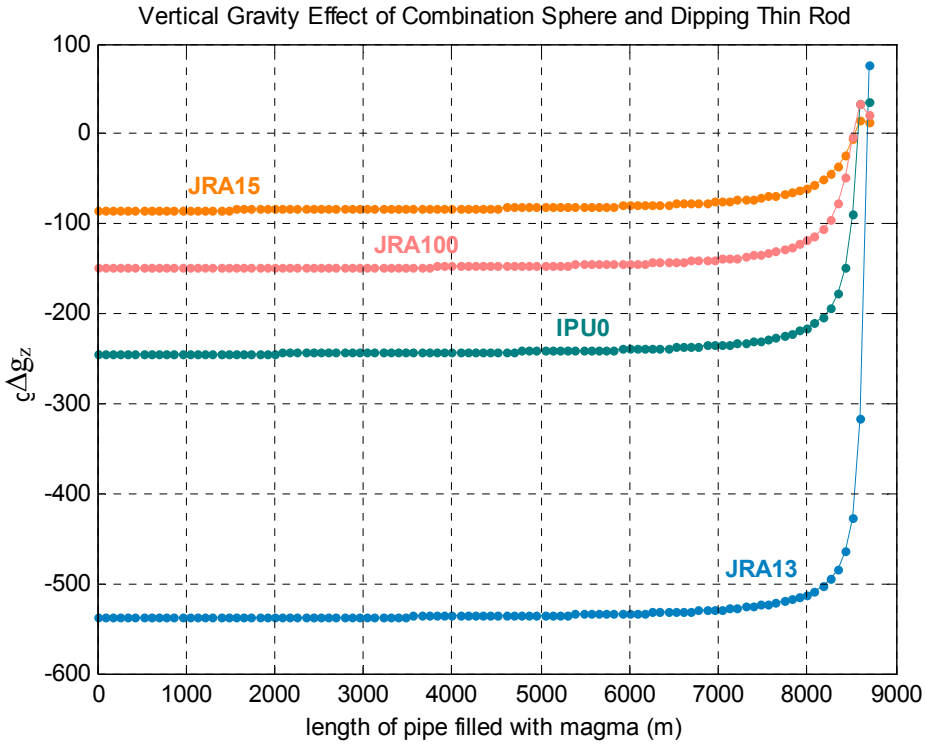


Fig.4.11. Vertical gravity effect of a pipe filled with magma at different levels at the stations JRA15, JRA13, IPU0, and JRA100; the top of the pipe is near JRAK13.

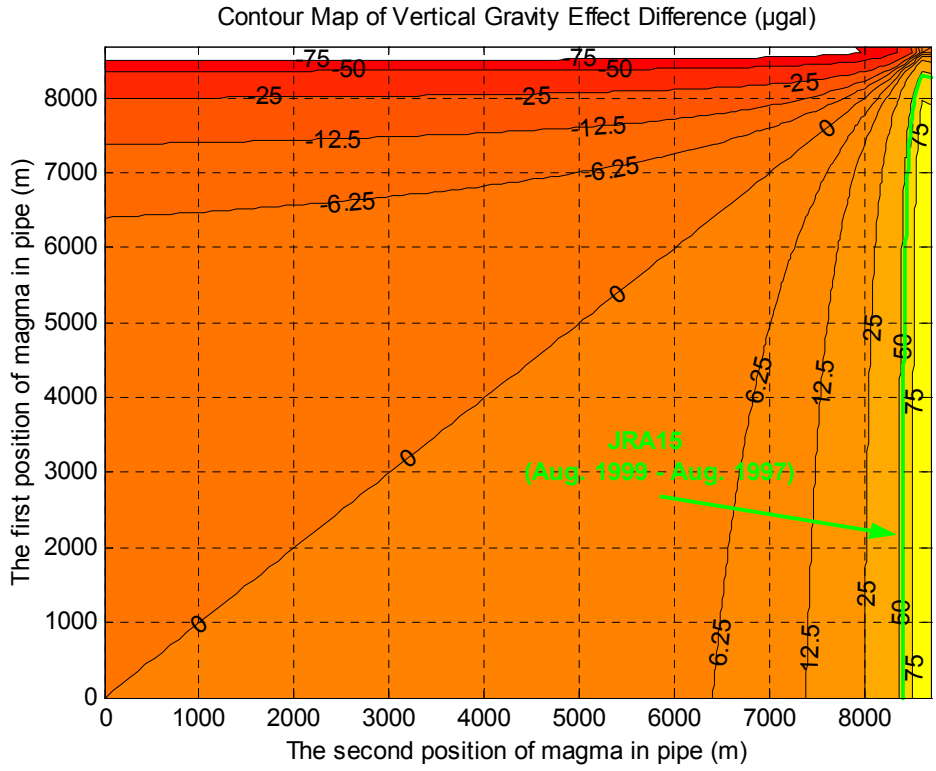


Fig.4.12. Contour map of vertical gravity effects dependent on magma height changes in the pipe at station JRA15; the green line represents the observed gravity changes between campaigns August 1999 and August 1997.

## 4.2.2. Combination-model: sphere and vertical thick cylinder

A thick cylinder (equation 4.16) represents the volcano better than a vertical thin rod (equation 4.2). Therefore the thin rod was replaced by a vertical thick cylinder in the combination model. Similar to the model in 4.2.1 we have to calculate (fig. 4.13) now:

- The vertical gravity effect of sphere filled with magma using (4.1).
- The vertical gravity effect of vertical thick cylinder.

We have to distinguish between different cases dependent on the altitude z (see fig. 4.13) of the observation point and the depth of the thick cylinder filled with magma $z_b$:

**If $z_b > z$**

- Vertical gravity effect of the vertical thick cylinder filled with magma

$$\Delta g_{z,cyl-m} = \frac{\partial \upsilon_{cyl-m}}{\partial z} = \pi R^2 G \Delta\rho \sum_{n=0}^{\infty} \frac{\left(\frac{1}{4}\right)_n \left(\frac{3}{4}\right)_n}{(1)_n (2)_n} \left[\varphi_n(z_m - l_m) - \varphi_n(z_m + l_m)\right] \qquad (4.18a)$$

where $\varphi_n(z_m) = \frac{1}{\sqrt{z_m{}^2 + X^2 + R^2}} \left[\frac{4R^2X^2}{\left(z_m{}^2 + X^2 + R^2\right)}\right]^n \sum_{k=0}^{\infty} \frac{\left(2n+\frac{1}{2}\right)_k}{(n+2)_k} \left(\frac{R^2}{z_m{}^2 + X^2 + R^2}\right)^k$

$\upsilon_{cyl\text{-}m}$ = gravitational potential of cylinder filled with magma

$\Delta g_{z,cyl\text{-}m}$ = vertical component of the gravitational attraction of a vertical cylinder filled with magma at any point

$(x)_n$ = $x(x+1)(x+2)(x+3) \ldots (x+n-1)$

$R$ = radius of the cylinder (m)
$X$ = horizontal distance between the centre of the cylinder and point P (m)
$z_m$ = vertical distance between the centre of the cylinder filled with magma and point P (m)
$2l_m$ = height of the cylinder filled with magma (m)

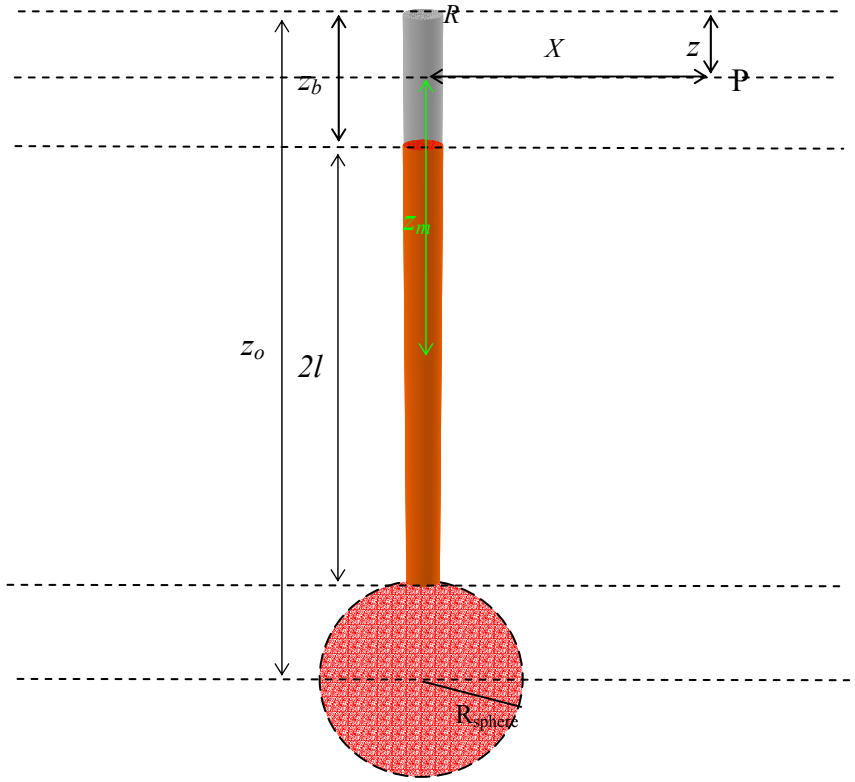


Fig.4.13. Combination model of sphere and vertical thick cylinder.

- Vertical gravity effect of the vertical thick cylinder filled with air

$$\Delta g_{z,cyl-a} = \frac{\partial \upsilon_{cyl-a}}{\partial z} = \pi R^2 G \Delta\rho \sum_{n=0}^{\infty} \frac{\left(\frac{1}{4}\right)_n \left(\frac{3}{4}\right)_n}{(1)_n (2)_n} \left[\varphi_n(z_a - l_a) - \varphi_n(z_a + l_a)\right] \qquad (4.18c)$$

where

$$\varphi_n(z_a) = \frac{1}{\sqrt{z_a{}^2 + X^2 + R^2}} \left[\frac{4R^2X^2}{\left(z_a{}^2 + X^2 + R^2\right)}\right]^n \sum_{k=0}^{\infty} \frac{\left(2n + \frac{1}{2}\right)_k}{(n+2)_k} \left(\frac{R^2}{z_a{}^2 + X^2 + R^2}\right)^k$$

In this case, we split the integration boundaries:
The parameters of a vertical thick cylinder below z are:
- $l_a = (z_b - z)/2$
- $z_a = l_a$

The parameters of vertical thick cylinder above z are:
- $l_a = z/2$
- $z_a = l_a$

**If $z_b \leq z$**

- Vertical gravity effect of the vertical thick cylinder filled with magma is given in equation 4.18a.
  In this case, we split again the integration boundaries:
  The parameters of vertical thick cylinder below z are:
  $l_m = (z_o - R)/2$
  $z_m = l_m$

  The parameters of vertical thick cylinder above z are:
  $l_m = (z - z_b)/2$
  $z_m = l_m$
  The sign of gravity effect of vertical thick cylinder above z is negative.

- Vertical gravity effect of the vertical thick cylinder filled with air is given in equation 4.17b
  where:
  $l_a = z_b/2$
  $z_a = z - l_a$
  For cylinders above z, the sign of vertical gravity effect is negative.

The name of the program is grav_sphere_cyl.m (appendix A.9). Examples are shown in chapter 7.

### 4.2.3. Gravity changes due to groundwater changes

Changes in the hydrothermal system of a volcano can be recorded by observing gravity changes. Porous volumes are filled by ground- or meteoric water. To estimate this effects the volcano is modeled as a system of concentric cylinders with different densities (fig. 4.14). The density changes ($\Delta\rho_1$, $\Delta\rho_2$, $\Delta\rho_3$, $\Delta\rho_4$...) due to changes of the water content in the cylinders can be determined by any optimizing estimator as least squares (Menke, 1984). Ready to use computer programs can be found in the optimization toolbox of MATLAB (http://www.mathworks.com).

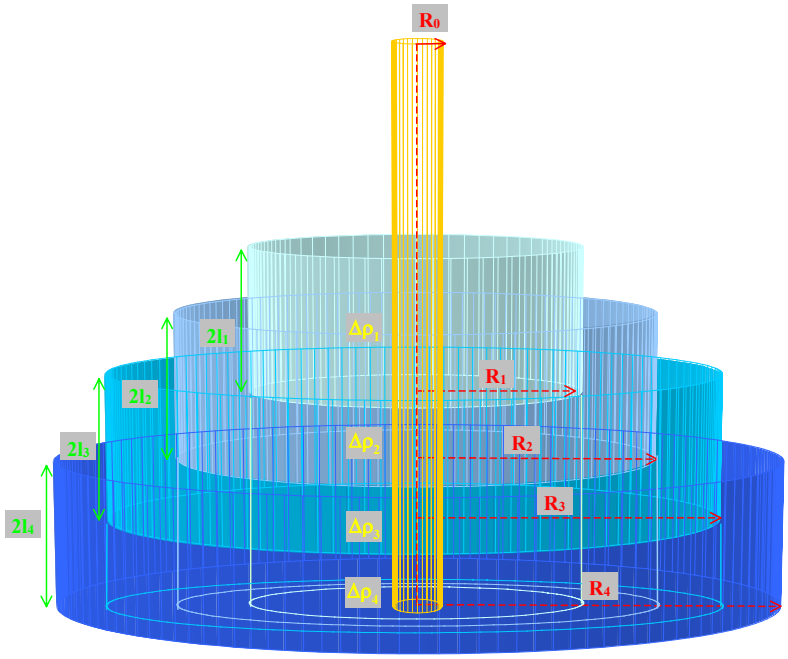


Fig. 4.14. Groundwater layers (hydrothermal system) around Merapi modeled with thick vertical cylinders of different densities.

The vertical gravity attraction of cylinder 1 at observation point P is calculated according (4.16)

$$\Delta g_{z,cyl-1} = \pi R_1^{\,2} G \Delta\rho_1 \sum_{n=0}^{\infty} \frac{\left(\frac{1}{4}\right)_n \left(\frac{3}{4}\right)_n}{(1)_n (2)_n} \left[\varphi_n(z_1 - l_1, R_1) - \varphi_n(z_1 + l_1, R_1)\right] - \pi R_0^{\,2} G \Delta\rho_1 \sum_{n=0}^{\infty} \frac{\left(\frac{1}{4}\right)_n \left(\frac{3}{4}\right)_n}{(1)_n (2)_n} \left[\varphi_n(z_1 - l_1, R_0) - \varphi_n(z_1 + l_1, R_0)\right] \tag{4.19a}$$

where

$$\varphi_n(z_1-l_1,R_1)=\frac{1}{\sqrt{(z_1-l_1)^2+X^2+{R_1}^2}}\left[\frac{4{R_1}^2X^2}{\left((z_1-l_1)^2+X^2+{R_1}^2\right)}\right]^n\cdot \sum_{k=0}^{\infty}\frac{\left(2n+\frac{1}{2}\right)_k}{(n+2)_k}\left(\frac{{R_1}^2}{(z_1-l_1)^2+X^2+{R_1}^2}\right)^k \tag{4.19b}$$

$$\varphi_n(z_1-l_1,R_0)=\frac{1}{\sqrt{(z_1-l_1)^2+X^2+{R_0}^2}}\left[\frac{4{R_0}^2X^2}{\left((z_1-l_1)^2+X^2+{R_0}^2\right)}\right]^n\cdot \sum_{k=0}^{\infty}\frac{\left(2n+\frac{1}{2}\right)_k}{(n+2)_k}\left(\frac{{R_0}^2}{(z_1-l_1)^2+X^2+{R_0}^2}\right)^k$$

or

$$\Delta g_{z,cyl-1}=\Delta\rho_1\left(\psi_1-\psi_1'\right) \tag{4.19c}$$

where

$$\psi_1=\pi{R_1}^2G\sum_{n=0}^{\infty}\frac{\left(\frac{1}{4}\right)_n\left(\frac{3}{4}\right)_n}{(1)_n(2)_n}\left[\varphi_n(z_1-l_1,R_1)-\varphi_n(z_1+l_1,R_1)\right]$$

$$\psi_1'=\pi{R_0}^2G\sum_{n=0}^{\infty}\frac{\left(\frac{1}{4}\right)_n\left(\frac{3}{4}\right)_n}{(1)_n(2)_n}\left[\varphi_n(z_1-l_1,R_0)-\varphi_n(z_1+l_1,R_0)\right] \tag{4.19d}$$

Equation 4.19c is used to calculate the vertical gravity effect for each cylinder as

$$\begin{aligned}
&\Delta g_{z,cyl-1}=\Delta\rho_1\left(\psi_1-\psi_1'\right)\\
&\Delta g_{z,cyl-2}=\Delta\rho_2\left(\psi_2-\psi_2'\right)\\
&\Delta g_{z,cyl-3}=\Delta\rho_3\left(\psi_3-\psi_3'\right)\\
&\vdots\\
&\Delta g_{z,cyl-k}=\Delta\rho_k\left(\psi_k-\psi_k'\right)
\end{aligned} \tag{4.20}$$

We obtain j equations for j observations point as

$$\begin{aligned}
\Delta g_{obs-1}&=\Delta\rho_1\left(\psi_{11}-\psi_{11}'\right)+\Delta\rho_2\left(\psi_{12}-\psi_{12}'\right)+\Delta\rho_3\left(\psi_{13}-\psi_{13}'\right)+\ldots+\Delta\rho_k\left(\psi_{1k}-\psi_{1k}'\right)\\
\Delta g_{obs-2}&=\Delta\rho_1\left(\psi_{21}-\psi_{21}'\right)+\Delta\rho_2\left(\psi_{22}-\psi_{22}'\right)+\Delta\rho_3\left(\psi_{23}-\psi_{23}'\right)+\ldots+\Delta\rho_k\left(\psi_{2k}-\psi_{2k}'\right)\\
\Delta g_{obs-3}&=\Delta\rho_1\left(\psi_{31}-\psi_{31}'\right)+\Delta\rho_2\left(\psi_{32}-\psi_{32}'\right)+\Delta\rho_3\left(\psi_{33}-\psi_{33}'\right)+\ldots+\Delta\rho_k\left(\psi_{3k}-\psi_{3k}'\right)\\
&\vdots\\
\Delta g_{obs-j}&=\Delta\rho_1\left(\psi_{j1}-\psi_{j1}'\right)+\Delta\rho_2\left(\psi_{j2}-\psi_{j2}'\right)+\Delta\rho_3\left(\psi_{j3}-\psi_{j3}'\right)+\ldots+\Delta\rho_k\left(\psi_{jk}-\psi_{jk}'\right)
\end{aligned} \tag{4.21}$$

or in matrix form:

$$\begin{bmatrix} \Delta g_{obs-1} \\ \Delta g_{obs-2} \\ \Delta g_{obs-3} \\ \vdots \\ \Delta g_{obs-j} \end{bmatrix} = \begin{bmatrix} \psi_{11}-\psi'_{11} & \psi_{12}-\psi'_{12} & \psi_{13}-\psi'_{13} & \cdots & \psi_{1k}-\psi'_{1k} \\ \psi_{21}-\psi'_{21} & \psi_{22}-\psi'_{22} & \psi_{23}-\psi'_{23} & \cdots & \psi_{2k}-\psi'_{2k} \\ \psi_{31}-\psi'_{31} & \psi_{32}-\psi'_{32} & \psi_{33}-\psi'_{33} & \cdots & \psi_{3k}-\psi'_{3k} \\ \vdots & \vdots & \vdots & \vdots & \vdots \\ \psi_{j1}-\psi'_{j1} & \psi_{j2}-\psi'_{j2} & \psi_{j3}-\psi'_{j3} & \cdots & \psi_{jk}-\psi'_{jk} \end{bmatrix} \begin{bmatrix} \Delta\rho_1 \\ \Delta\rho_2 \\ \Delta\rho_3 \\ \vdots \\ \Delta\rho_k \end{bmatrix} \tag{4.22}$$

or

$$\mathbf{d} = \mathbf{C}\,\mathbf{x} \tag{4.23}$$

with:

$$\mathbf{d} = \begin{bmatrix} \Delta g_{obs-1} \\ \Delta g_{obs-2} \\ \Delta g_{obs-3} \\ \vdots \\ \Delta g_{obs-j} \end{bmatrix},$$

$$\mathbf{C} = \begin{bmatrix} \psi_{11}-\psi'_{11} & \psi_{12}-\psi'_{12} & \psi_{13}-\psi'_{13} & \cdots & \psi_{1k}-\psi'_{1k} \\ \psi_{21}-\psi'_{21} & \psi_{22}-\psi'_{22} & \psi_{23}-\psi'_{23} & \cdots & \psi_{2k}-\psi'_{2k} \\ \psi_{31}-\psi'_{31} & \psi_{32}-\psi'_{32} & \psi_{33}-\psi'_{33} & \cdots & \psi_{3k}-\psi'_{3k} \\ \vdots & \vdots & \vdots & \vdots & \vdots \\ \psi_{j1}-\psi'_{j1} & \psi_{j2}-\psi'_{j2} & \psi_{j3}-\psi'_{j3} & \cdots & \psi_{jk}-\psi'_{jk} \end{bmatrix},$$

$$\mathbf{x} = \begin{bmatrix} \Delta\rho_1 \\ \Delta\rho_2 \\ \Delta\rho_3 \\ \vdots \\ \Delta\rho_k \end{bmatrix}$$

According (Menke, 1984) the solution of the least squares problem ($L_2$-norm) is

$$\min_x f(x) = \min_x \frac{1}{2}\left\|Cx-d\right\|_2^2 = \min_x \frac{1}{2}\sum\left|C_j x_j - d_j\right|^2,$$

with
- $j$ = number of equations,
- $k$ = number of variables.

The solution of the function is $x = C \setminus d$ (syntax in MATLAB).

If we have constraints, constraint linear least squares estimators as

$$\min_x f(x) = \min_x \frac{1}{2}\left\|Cx-d\right\|_2^2$$

can be applied, where the solution is determined in such way that

$$A.x \leq b,$$
$$Aeg \,.\, x = beg,$$
$$lb \leq x \leq ub.$$

The solution x can be found with the MATLAB procedure lsqlin according

$$x = lsqlin(C,d,A,b,Aeg,beg,lb,ub)$$

or

$$x = lsqlin(C,d,A,b,Aeg,beg,lb,ub,x0)$$

where the starting point is set to x0.
The meanings of the parameters are:

A, b : The matrix A and vector b are, respectively, the coefficients of the linear inequality constraints and the corresponding right-hand side vector: **A.x** ≤ **b**.

Aeq, beq : The matrix Aeq and vector beq are, respectively, the coefficients of the linear equality constraints and the corresponding right-hand side vector: **Aeq . x** = **beq**.

C, d : The matrix C and vector d are, respectively, the coefficients of the over- or under-determined linear system and the right-hand-side vector to be solved.

lb, ub : Lower and upper bound vectors (or matrices). The arguments are normally the same size as x. However, if lb has fewer elements than x, say only m, then only the first m elements in x are bounded below; upper bounds in ub can be defined in the same manner. Unbounded variables may also be specified using -Inf (for lower bounds) or Inf (for upper bounds). For example, if lb (i) = -∞ then the variable x (i) is unbounded below.

As constraints the reliable density changes are introduced. As lower boundaries lb = -50 kg/m$^3$ as upper ub = +50 kg/m$^3$ were chosen.